Trivariate Optimal Smoothing Splines with Dynamic Shape Modeling of Deforming Object

Hiroyuki Kano * Hiroyuki Fujioka **

Division of Science, Tokyo Denki University, Saitama 350-0394, JAPAN (e-mail: kano@mail.dendai.ac.jp)
**Department of System Management, Fukuoka Institute of Technology, Fukuoka 811-0295, JAPAN (e-mail: fujioka@fit.ac.jp).*

Abstract: We develop a method of constructing trivariate optimal smoothing splines using normalized uniform B-spline as the basis functions. Such splines are useful particularly for modeling dynamic shape of 3-dimensional deformable object by using two variables for 3D shape and one for time evolution. The trivariate splines are constructed as a tensor product of three B-splines, and an optimal smoothing spline problem is solved together with typical examples of constraints as periodicity. The problem is formulated as convex quadratic programming (QP) problem in such a way that 3D array of control points is vectorized and a MATLAB QP solver is readily applicable for numerical solutions. We demonstrate usefulness of the method by dynamic shape modeling of red blood cell, where we will see that relatively small number of observation data yield satisfactory results.

Keywords: Splines; Smoothing; Trivariate splines; Dynamic shape modeling; Red blood cell.

1. INTRODUCTION

We consider optimal trivariate splines and develop practical algorithm for numerical computations. There have been numerous studies on splines in single variable and their theories and algorithms as interpolation and approximation or smoothing, have been extended to splines in two variables (bivariate splines). They have been shown very useful in various fields of science and engineering as computer graphics, numerical analysis, image processing, trajectory planning, statistical data analysis, etc. Obviously, one is interested in extending those theories and algorithms to the case of three variables and moreover to the general case of n-variate splines. Such extensions are desired in many applications as aforementioned area in general, and here we consider modeling of 3D shape of deformable objects.

Typical objects with such deformable motions may be wet material object – such as jellyfish, red blood cell and amoeba, etc. One of important issues in their studies is to analyze and understand the motions of such objects from the observational data, e.g. image frames in a movie file. The contour modeling of objects then plays key roles and have been studied in the field of image processing, and various techniques, e.g. active contour model (Blake [2000], Brigger [2000]), have been developed. The approach in these studies is to treat the contours independently at each sampling time and hence is not suitable to analyze and understand a whole motion of the deformable objects continuously in time.

Another applications related to our present study are the spline-based solid modeling of the human organs from a set of tomograph data obtained, for instance, by the magnetic range imaging (MRI) (Amini [2001], Ameur [2007]). Human lungs are modeled by periodic smoothing spline surface (Jaillet [1997]), where a set of contours are designed first from tomograph data and then a spline surface (bivariate spline) is designed from the contours. The design method of smoothing spline surfaces is thus viewed as a two step procedure, and we may point out that the whole set of tomograph data is not used effectively to construct the spline surface. Also, a similar idea has been applied to the 3-dimensional shape modeling of cell nucleus (Peng [2011]).

As for the theories and algorithms of multi-variable splines, there are some literatures: Trivariate splines are used to model 3D shapes using triangle mesh of geometric shapes as the input data (Martin [2009]). Also an interpolation problem is considered for multi-dimensional splines restricting to only cubic splines (Habermann [2007]). Another approach to splines is by the so-called dynamic splines, where linear control systems are used as spline generator. The book (Egerstedt [2010]) contains the state of the art of dynamic splines, and the authors developed a theory of periodic splines based on Hilbert space optimization (Kano [2008]). This method has the advantage in that various types of functions can be used as basis functions as exponential functions, trigonometric functions, polynomials, and their combinations by choosing appropriate system matrix. However, extension to multi-variable case is not easy by this approach.

Here we develop a method for constructing optimal trivariate smoothing splines using tensor product of three B-splines as the basis elements. In particular, normalized uni-

form B-splines (Kano [2005a]) are used, which enable us to derive concise representation of optimal smoothing splines and to incorporate various types of constraints more easily. Included in the constraints are periodicity as treated in this paper as well as the so-called shape preserving splines as monotone splines, convex splines, constraints on integral values, and so forth (Kano [2011], Fujioka [2011]). This paper extends our B-spline based studies on optimal splines, in particular those in (Kano [2005b], Fujioka [2009]), and the theories and algorithms are developed so that the n-variate case is deduced. The splines treated are of arbitrary degree. The problem is formulated as convex quadratic programming (QP) problem in such a way that 3D array of control points is vectorized and a MATLAB QP solver is readily applicable for numerical solutions. Trivariate smoothing splines are useful to dynamic shape modeling of deforming objects, where two variables are used to model the 3D shape imposing periodicity and the other to represent time evolution. Here we consider modeling red blood cell (Karlsson [2005], Pozrikidis [2003]), and we will see that relatively small number of observation data consisting of time sequence of 2D data sets yield satisfactory results.

Note that, by restricting to tensor product construction of B-splines with uniform knot point distribution (cf. (Lai [2007], Anderson [1993]), we could derive concise expressions for trivariate smoothing splines with various constraints, readily implementable as computational algorithms. Moreover, they can be used systematically and effectively in problems as dynamic 3D shape modeling, which is novel to the authors knowledge.

This paper is organized as follows. In Section 2, we formulate and solve the problems of optimal design of trivariate smoothing splines. Periodicity is considered in Section 3. In Section 4, the results are applied to dynamic shape modeling of red blood cell, and concluding remarks are given in Section 5.

2. TRIVARIATE OPTIMAL SMOOTHING SPLINES

We describe a problem of optimal design of trivariate smoothing splines and derive the solution.

2.1 Trivariate Spline by B-Splines

For designing trivariate splines $x(t)$, $t = (t_1, t_2, t_3)$, we employ normalized, uniform B-spline function $B_k(s)$ of degree k as the basis functions,

$$x(t) = \sum_{i_1=-k}^{m_1-1} \sum_{i_2=-k}^{m_2-1} \sum_{i_3=-k}^{m_3-1} \tau_{i_1,i_2,i_3} B_{k,i_1}^{[1]}(t_1) B_{k,i_2}^{[2]}(t_2) B_{k,i_3}^{[3]}(t_3),$$

(1)

where $m_i(> 2)$ are integers, τ_{i_1,i_2,i_3} are the control points, and $B_{k,i}^{[j]}(\cdot)$ are the scaled and shifted B-splines of degree k with knot points $u_i^{[j]}$ defined by

$$B_{k,i}^{[j]}(s) = B_k(\alpha_j(s - u_i^{[j]})), \ j = 1, 2, 3.$$

(2)

Here $\alpha_j(> 0)$ are the scaling factors, and specify the intervals of equally spaced knot points as

$$u_{i+1}^{[j]} - u_i^{[j]} = \frac{1}{\alpha_j}.$$

(3)

Note that, here and hereafter, the superscript $[j]$ is used to refer j-th variable t_j for $j = 1, 2, 3$.

For convenience, the definition of normalized, uniform B-spline functions $B_k(s)$ used in above is given.

$$B_k(s) = \begin{cases} N_{k-j,k}(s - j) & j \le s < j+1 \ \ j = 0, \cdots, k \\ 0 & s < 0, \ k+1 \le s. \end{cases}$$

(4)

Here the basis elements $N_{j,k}(s)$ $(j = 0, 1, \cdots, k)$ are obtained recursively by the following algorithm (Boor [2001]). Let $N_{0,0}(s) \equiv 1$ and, for $i = 1, 2, \cdots, k$, compute

$$\begin{cases} N_{0,i}(s) = \dfrac{1-s}{i} N_{0,i-1}(s) \\ N_{j,i}(s) = \dfrac{i-j+s}{i} N_{j-1,i-1}(s) \\ \qquad + \dfrac{1+j-s}{i} N_{j,i-1}(s), \ j = 1, \cdots, i-1 \\ N_{i,i}(s) = \dfrac{s}{i} N_{i-1,i-1}(s). \end{cases}$$

(5)

Thus, $B_k(s)$ is a piece-wise polynomial of degree k with integer knot points and is $k - 1$ times continuously differentiable, and it holds that $\sum_{j=0}^{k} N_{j,k}(s) = 1$, $0 \le s \le 1$.

2.2 Optimal Smoothing Splines

First we formulate a problem of trivariate optimal smoothing splines and then present its solution. Note that the problem described in this section is usually solved in conjunction with the constraints as given in Section 3.

By choosing appropriate control points τ_{i_1,i_2,i_3}, the function $x(t)$ in (1) represents trivariate spline of degree k on the domain $\mathcal{S} = I_1 \times I_2 \times I_3 \subset \mathbf{R}^3$ where $I_j = [u_0^{[j]}, u_{m_j}^{[j]}]$. Now suppose that a set of data

$$\mathcal{D} = \Big\{ (v_i; d_i) : v_i = (v_i^{[1]}, v_i^{[2]}, v_i^{[3]}) \in \mathcal{S}, \ d_i \in \mathbf{R}, $$
$$i = 1, 2, \cdots, N \Big\}$$

(6)

is given, and let $\tau \in \mathbf{R}^{M_1 \times M_2 \times M_3}$ with $M_i = m_i + k$.

Then, a standard problem of designing optimal trivariate smoothing splines is to find a function $x(t)$, or equivalently an array $\tau \in \mathbf{R}^{M_1 \times M_2 \times M_3}$, minimizing the following cost function consisting of a smoothness term and approximation error term.

Problem 1. Construct the spline $x(t)$ in (1) such that

$$\min_{\tau \in \mathbf{R}^{M_1 \times M_2 \times M_3}} J(\tau),$$

where

$$J(\tau) = \lambda \int_{\mathcal{S}} \left(\nabla^2 x(t) \right)^2 dt + \sum_{i=1}^{N} w_i (x(v_i) - d_i)^2. \quad (7)$$

In (7), $\lambda(> 0)$ is a smoothing parameter, $\nabla^2 = \frac{\partial^2}{\partial t_1^2} + \frac{\partial^2}{\partial t_2^2} + \frac{\partial^2}{\partial t_3^2}$ and w_i $(0 < w_i \le 1)$ denotes weights for approximation errors.

This problem can be solved as follows. First, we express the right hand side of (7) in terms of τ. Let $b_j(s) \in \mathbf{R}^{M_j}$ $(j = 1, 2, 3)$ be

$$b_j(s) = \left[B^{[j]}_{k,-k}(s) \ B^{[j]}_{k,-k+1}(s) \ \cdots \ B^{[j]}_{k,m_j-1}(s) \right]^T$$
$$= \left[B_k(\alpha_j(s - u^{[j]}_{-k})) \ B_k(\alpha_j(s - u^{[j]}_{-k+1})) \right.$$
$$\left. \cdots \ B_k(\alpha_j(s - u^{[j]}_{m_j-1})) \right]^T . (8)$$

Moreover, the three dimensional array $\tau \in \mathbf{R}^{M_1 \times M_2 \times M_3}$ is reshaped into a one dimensional, column vector form $\hat{\tau} \in \mathbf{R}^M$ with $M = M_1 M_2 M_3$ according to the following rule.

Procedure 1. Three-dimensional array $A = [a_{i_1,i_2,i_3}] \in \mathbf{R}^{M_1 \times M_2 \times M_3}$ is vectorized as $\hat{A} \in \mathbf{R}^M$ ($M = M_1 M_2 M_3$) so that the j-th element $\hat{A}_j$ of $\hat{A}$ is defined by

$$j = 0$$
$$for \ \ i_3 = 1 : M_3$$
$$for \ \ i_2 = 1 : M_2$$
$$for \ \ i_1 = 1 : M_1$$
$$j = j + 1$$
$$\hat{A}_j = a_{i_1,i_2,i_3}$$
$$end$$
$$end$$
$$end$$

We denote this construction of vector $\hat{A}$ from the array A as $\hat{A} = \text{vec} \ A$, and the control point vector $\hat{\tau}$ is obtained as

$$\hat{\tau} = \text{vec} \ \tau. \qquad (9)$$

Remark 1. This definition of 'vec' operation may be regarded as a natural extension of the well-known definition of vec-function for matrices (see e.g. Lancaster [1985]). Namely, for a matrix $A = [a_1 \ a_2 \cdots \ a_{M_2}] \in \mathbf{R}^{M_1 \times M_2}$ with $a_i \in \mathbf{R}^{M_1}$, the vector vec A is defined as vec $A = \left[a_1^T \ a_2^T \ \cdots \ a_{M_2}^T \right]^T \in \mathbf{R}^{M_1 M_2}$, and this vectorization process agrees with that in Procedure 1 when the outer loop on i_3 is deleted for two dimensional array.

Remark 2. Using MATLAB function 'reshape', the vector $\hat{\tau}$ is obtained from the array τ by $\hat{\tau} = \text{reshape}(\tau, M, 1)$, and conversely $\tau = \text{reshape}(\hat{\tau}, M_1, M_2, M_3)$.

Now we get the following formula for $x(t)$, where $\otimes$ denotes Kronecker product.

Proposition 1. Trivariate spline $x(t)$ in (1) is expressed as

$$x(t) = b^T(t)\hat{\tau}, \qquad (10)$$

where $b(t) \in \mathbf{R}^M$ is defined by

$$b(t) = b_3(t_3) \otimes b_2(t_2) \otimes b_1(t_1). \qquad (11)$$

The cost function in (7) is then obtained in terms of $\hat{\tau}$ as

$$J(\hat{\tau}) = \lambda \hat{\tau}^T Q \hat{\tau} + \left(B^T \hat{\tau} - d \right)^T W \left(B^T \hat{\tau} - d \right). \qquad (12)$$

Here, $Q \in \mathbf{R}^{M \times M}$ is a Gram matrix defined by

$$Q = \int_{\mathcal{S}} \left(\nabla^2 b(t) \right) \left(\nabla^2 b(t) \right)^T dt, \qquad (13)$$

and obviously $Q = Q^T \geq 0$. The Laplace operator ∇^2 on vector $b(t)$ should be understood as operating on each element of the vector. Moreover, in (12), matrix $B \in \mathbf{R}^{M \times N}$ is defined by

$$B = [\, b(v_1) \ b(v_2) \ \cdots \ b(v_N) \,]$$
$$= \left[b_3(v_1^{[3]}) \otimes b_2(v_1^{[2]}) \otimes b_1(v_1^{[1]}) \right.$$
$$\left. \cdots \ b_3(v_N^{[3]}) \otimes b_2(v_N^{[2]}) \otimes b_1(v_N^{[1]}) \right], \quad (14)$$

and $W \in \mathbf{R}^{N \times N}$ and $d \in \mathbf{R}^N$ by

$$W = \text{diag} \, \{ \, w_1 \ w_2 \ \cdots \ w_N \, \}$$
$$d = [\, d_1 \ d_2 \ \cdots \ d_N \,]^T. \qquad (15)$$

Thus, the cost function in (12) is expressed as

$$J(\hat{\tau}) = \hat{\tau}^T G \hat{\tau} - 2g^T \hat{\tau} + c, \qquad (16)$$

where

$$G = \lambda Q + BWB^T, \quad g = BWd, \quad c = d^T Wd, \qquad (17)$$

and the optimal smoothing spline is obtained as a solution of

$$G\hat{\tau} = g. \qquad (18)$$

Finally in this section, we consider the Gram matrix Q in (13) from its computational point of view. Noting that

$$\nabla^2 b(t) = \left(\frac{\partial^2}{\partial t_1^2} + \frac{\partial^2}{\partial t_2^2} + \frac{\partial^2}{\partial t_3^2} \right) (b_3(t_3) \otimes b_2(t_2) \otimes b_1(t_1))$$
$$(19)$$

and using the properties of Kronecker products $(A \otimes B \otimes C)^T = A^T \otimes B^T \otimes C^T$, $(A \otimes B \otimes C)(A' \otimes B' \otimes C') = (AA') \otimes (BB') \otimes (CC')$ for matrices of compatible dimensions, we obtain

$$Q = Q_3^{(22)} \otimes Q_2^{(00)} \otimes Q_1^{(00)} + Q_3^{(20)} \otimes Q_2^{(02)} \otimes Q_1^{(00)}$$
$$+ Q_3^{(20)} \otimes Q_2^{(00)} \otimes Q_1^{(02)} + Q_3^{(02)} \otimes Q_2^{(20)} \otimes Q_1^{(00)}$$
$$+ Q_3^{(00)} \otimes Q_2^{(22)} \otimes Q_1^{(00)} + Q_3^{(00)} \otimes Q_2^{(20)} \otimes Q_1^{(02)}$$
$$+ Q_3^{(02)} \otimes Q_2^{(00)} \otimes Q_1^{(20)} + Q_3^{(00)} \otimes Q_2^{(02)} \otimes Q_1^{(20)}$$
$$+ Q_3^{(00)} \otimes Q_2^{(00)} \otimes Q_1^{(22)}. \qquad (20)$$

Here $Q_l^{(ij)} \in \mathbf{R}^{M_l \times M_l}$ ($l = 1, 2, 3; \ i, j = 0, 1, 2$) are defined by

$$Q_l^{(ij)} = \int_{I_l} \frac{d^i b_l(s)}{ds^i} \frac{d^j b_l^T(s)}{ds^j} ds \qquad (21)$$

and hence $Q_l^{(ji)} = (Q_l^{(ij)})^T$ holds. The elements of $Q_l^{(ij)}$ can be precomputed from the B-splines once the parameters k and m_l are determined (see Fujioka [2005] for the cubic spline case $k = 3$).

3. PERIODICITY

There are various types of constraints that we would like to impose on smoothing splines $x(t)$. Here we consider the case of periodicity.

3.1 t_3-periodicity

For convenience of description, we start with the spline $x(t_1, t_2, t_3)$ which is periodic in the third variable t_3, referring it as t_3-periodic. Specifically, recalling that the spline $x(t_1, t_2, t_3)$ is defined for $t_j \in I_j = [u_0^{[j]}, u_{m_j}^{[j]}]$ ($j =$

1, 2, 3), the spline $x(t_1, t_2, t_3)$ is t_3-periodic if it satisfies the constraint

$$\frac{\partial^l}{\partial t_3^l} x(t_1, t_2, u_0^{[3]}) = \frac{\partial^l}{\partial t_3^l} x(t_1, t_2, u_{m_3}^{[3]}) \qquad (22)$$

for $\forall t_1 \in I_1, \forall t_2 \in I_2$ and $\forall l = 0, 1, \cdots, k-1$. This t_3-periodicity of $x(t_1, t_2, t_3)$ should be understood as that it is periodic in t_3 with the period $u_{m_3}^{[3]} - u_0^{[3]}$ if its domain $I_1 \times I_2 \times I_3$ is extended in the entire t_3-axis, namely in $I_1 \times I_2 \times (-\infty, +\infty)$.

By introducing a matrix $T_i \in \mathbf{R}^{M_1 \times M_2}$

$$T_i = [\tau_{i_1, i_2, i}]_{i_1, i_2 = -k}^{m_1 - 1, m_2 - 1} \qquad (23)$$

for $i = -k, -k+1, \cdots, m_3 - 1$ and its column vector expression $\hat{\tau}_i \in \mathbf{R}^{M_{12}}$ ($M_{12} = M_1 M_2$) (see Remark 1), i.e.

$$\hat{\tau}_i = \text{vec } T_i, \qquad (24)$$

the following relation holds for $\hat{\tau} \in \mathbf{R}^M$ given by (9)

$$\hat{\tau} = \begin{bmatrix} \hat{\tau}_{-k} \\ \hat{\tau}_{-k+1} \\ \vdots \\ \hat{\tau}_{m_3-1} \end{bmatrix} = \begin{bmatrix} \text{vec } T_{-k} \\ \text{vec } T_{-k+1} \\ \vdots \\ \text{vec } T_{m_3-1} \end{bmatrix}. \qquad (25)$$

We then get the following result.

Proposition 2. The spline $x(t_1, t_2, t_3)$ is t_3-periodic if and only if

$$\hat{\tau}_i = \hat{\tau}_{m_3+i}, \quad \forall i = -k, -k+1, \cdots, -1 \qquad (26)$$

holds for vectors $\hat{\tau}_i$ defined in (24).

Note that, in terms of the entire vector $\hat{\tau} \in \mathbf{R}^M$, the condition (26) is expressed from (25) as

$$C_3 \hat{\tau} = 0 \qquad (27)$$

where $C_3 \in \mathbf{R}^{kM_{12} \times M}$ ($M_{12} = M_1 M_2$) is defined by

$$C_3 = [\, I_{kM_{12}} \; O_{kM_{12}, M-2kM_{12}} \; -I_{kM_{12}} \,]. \qquad (28)$$

Thus t_3-periodic optimal smoothing spline is obtained by minimizing the cost (16) under the constraint (27).

3.2 t_2- and t_1-periodicity

For two vectors $p \in \mathbf{R}^m$ and $q \in \mathbf{R}^n$, we define a permutation matrix $K_{n,m} \in \mathbf{R}^{nm \times nm}$ such that

$$K_{n,m}(p \otimes q) = q \otimes p. \qquad (29)$$

Then it holds that $K_{n,m}^T = K_{n,m}^{-1} = K_{m,n}$ (see e.g. Magnus [1999]).

Now, t_2- and t_1-periodicity are defined similarly as in (22), and we get the following conditions. The latter case is put in parentheses.

Proposition 3. The spline $x(t_1, t_2, t_3)$ is t_2-periodic (t_1-periodic) if and only if

$$\hat{\tau}_i' = \hat{\tau}_{m_2+i}' \quad (\hat{\tau}_i'' = \hat{\tau}_{m_1+i}'') \quad \forall i = -k, -k+1, \cdots, -1 \quad (30)$$

holds, where the vectors $\hat{\tau}_i' \in \mathbf{R}^{M_{13}}$ with $M_{13} = M_1 M_3$ (the vectors $\hat{\tau}_i'' \in \mathbf{R}^{M_{23}}$ with $M_{23} = M_2 M_3$) are defined by partitioning a permuted $\hat{\tau}$ vector as

$$\hat{\tau}' = K_{M_{12}, M_3} \hat{\tau} = \begin{bmatrix} \hat{\tau}_{-k}' \\ \hat{\tau}_{-k+1}' \\ \vdots \\ \hat{\tau}_{m_2-1}' \end{bmatrix} \quad \left(\hat{\tau}'' = K_{M_1, M_{23}} \hat{\tau} = \begin{bmatrix} \hat{\tau}_{-k}'' \\ \hat{\tau}_{-k+1}'' \\ \vdots \\ \hat{\tau}_{m_1-1}'' \end{bmatrix} \right). \qquad (31)$$

In terms of the vector $\hat{\tau}$, the condition (30) for t_2-periodicity (t_1-periodicity) is given as

$$C_2 \hat{\tau} = 0 \quad (C_1 \hat{\tau} = 0) \qquad (32)$$

where $C_2 \in \mathbf{R}^{kM_{13} \times M}$ ($C_1 \in \mathbf{R}^{kM_{23} \times M}$) is defined by

$$C_2 = [\, I_{kM_{13}} \; O_{kM_{13}, M-2kM_{13}} \; -I_{kM_{13}} \,] K_{M_{12}, M_3}$$

$$(C_1 = [\, I_{kM_{23}} \; O_{kM_{23}, M-2kM_{23}} \; -I_{kM_{23}} \,] K_{M_1, M_{23}}) \quad (33)$$

Remark 3. From Proposition 2 and (25), we see that the condition for t_3-periodicity may be stated as $T_i = T_{m_3+i} \; \forall i \; (-k \le i \le -1)$. Likewise we can verify that t_2- and t_1-periodicity are equivalent to $T_i' = T_{m_2+i}'$ and $T_i'' = T_{m_1+i}'' \; \forall i \; (-k \le i \le -1)$, respectively, where

$$T_i' = [\tau_{i_1, i, i_3}]_{i_1, i_3 = -k}^{m_1 - 1, m_3 - 1}, \quad T_i'' = [\tau_{i, i_2, i_3}]_{i_2, i_3 = -k}^{m_2 - 1, m_3 - 1}. \quad (34)$$

In other words, the t_j-periodicity is achieved by equating the first and last k matrices constructed from τ_{i_1, i_2, i_3} with the j-th parameter fixed. Propositions 2 and 3, (27) and (32), are employed so that the conditions can be used directly in connection with the cost $J(\hat{\tau})$ in (16).

4. NUMERICAL EXPERIMENTS

We examine the performances of trivariate optimal smoothing splines numerically by modeling deformation of red blood cell.

First we summarize the numerical procedure for constructing the splines. The problem of optimal smoothing splines is formulated as a convex quadratic programming (QP) problem with the cost function given in the form

$$J(\hat{\tau}) = \hat{\tau}^T G \hat{\tau} - 2g^T \hat{\tau} + c, \qquad (35)$$

together with the constraints

$$C \hat{\tau} = 0. \qquad (36)$$

This constraint contains all the necessary equality constraints such as the periodicity as developed in the previous sections, and it can be assumed without loss of generality that the constraint matrix C is of row full rank. Efficient numerical tool is available for such a QP problem and here we use MATLAB function 'quadprog'.

In the following experiments, we use cubic splines ($k = 3$) and the so-called generalized cross validation (GCV) method (Wahba [1990]) for determining the smoothing parameter λ.

4.1 Deformation of Red Blood Cell

We examine 3D deformation motion of red blood cells by trivariate smoothing splines. The data $\mathcal{D}$ is obtained by sampling the following function

$$f(\theta, \phi, t) = \sqrt{h_1^2(\theta, \phi, t) + h_2^2(\theta, \phi, t) + h_3^2(\theta, \phi, t)} \quad (37)$$

where $\theta \in I_1 = [0, 2\pi]$ and $\phi \in I_2 = [0, 2\pi]$ and $t \in I_3 = [0, T]$ with $T = 10$ denotes time, and

$$h_1(\theta, \phi, t) = (a + 0.5 \cos(\omega t)) \alpha \sin \theta \cos \phi$$

$$h_2(\theta, \phi, t) = a \alpha \sin \theta \sin \phi$$

$$h_3(\theta, \phi, t) = (a + 0.5 \cos(\omega t)) \frac{\alpha}{2} (0.207 + 2.003 \sin^2 \theta$$

$$- 1.123 \sin^4 \theta) \cos \theta \qquad (38)$$

where $a = 2.8$, $\alpha = 1.38581894$ and $\omega = \pi/5$. This model is taken from (Pozrikidis [2003]), which we modified so as

to include the additional parameter t in order to generate deforming motion. Note that $f(\theta, \phi, t)$ is periodic in all the three variables. In Figure 1 (a), the function $f(\theta, \phi, t)$ at time $t = 0$ is plotted, and the corresponding 3D shape of red blood cell in $O - XYZ$ space is constructed by the following transformation of polar coordinate system

$$X(\theta, \phi, t) = f(\theta, \phi, t) \sin \theta \sin \phi$$
$$Y(\theta, \phi, t) = f(\theta, \phi, t) \sin \theta \cos \phi$$
$$Z(\theta, \phi, t) = f(\theta, \phi, t) \cos \theta. \qquad (39)$$

The data points $v_i = (v_i^{[1]}, v_i^{[2]}, v_i^{[3]})$ are taken as 3-dimensional lattice points, equally spaced in each axis with the number $N_1 = 5$, $N_2 = 5$, $N_3 = 10$ in θ, ϕ, t axes respectively. Hence the total number of data is $N = 250$, and the function is sampled to generate the data $d_i = f(v_i) + \epsilon_i$ with ϵ_i being 10% additive white Gaussian noise.

A trivariate optimal smoothing spline $x(\theta, \phi, t)$ is constructed under the periodicity constraints on all the variables θ, ϕ, t with the periods $2\pi, 2\pi$ and $T(= 10)$ respectively, where the method described in Section 3 is used. The number of control points are set as $m_1 = 10, m_2 = 10, m_3 = 15$, hence the knot point intervals along the θ, ϕ, t axes are $2\pi/m_1 \approx 0.628(= 1/\alpha_1)$, $2\pi/m_2 \approx 0.628(= 1/\alpha_2)$ and $10/m_3 \approx 0.667(= 1/\alpha_3)$, respectively. The weights w_i for approximation errors are set as $w_i = 1/N \; \forall i$.

By generalized cross validation method, the optimal value of the smoothing parameter is obtained as $\lambda^* = 6.3096 \times 10^{-6}$. We constructed trivariate optimal smoothing spline $x(\theta, \phi, t)$. The results are shown in Figure 2 as the 3D shapes of the red blood cell reconstructed in the $O - XYZ$ space by a polar coordinate transformation defined similarly as in (39). The shapes are plotted at the four time instants of continuous, periodic deforming motion reconstructed from $x(\theta, \phi, t)$.

We examined the approximation errors. Figure 3 (a) shows the error between the original function and constructed spline function $f(\theta, \phi, t) - x(\theta, \phi, t)$ at time $t = 0$, and error norms $\|f(\theta, \phi, t) - x(\theta, \phi, t)\|$ computed for each t are plotted in (b) (blue line), where matrix 2-norm is used. Also shown in (b) are the error norms for the case of increased number of data points with $N_1 = N_2 = 10, N_3 = 20$ ($N = 2000$, green line) and $N_1 = N_2 = 20, N_3 = 40$ ($N = 32000$, red line), and the norm of original function $f(\theta, \phi, t)$ (dotted line, right scale). Clearly increasing the number of data decreases approximation errors.

Figure 4 shows XY-plane profiles of 3D shapes of the red blood cell plotted at four time instants $t = 0, T/4, 2T/4$ and $t = 3T/4$ for two cases of data points: (a) $N_1 = N_2 = 5, N_3 = 10$ and (b) $N_1 = N_2 = 20, N_3 = 40$. The profiles obtained from the optimal spline $x(\theta, \phi, t)$ are shown in solid lines and those by original function $f(\theta, \phi, t)$ in dotted lines. We see that the profiles by splines agree quite well in (a) although the number of sampled data is relatively small, and agree very well in (b).

5. CONCLUDING REMARKS

We developed a method of constructing trivariate optimal smoothing splines using normalized uniform B-spline as
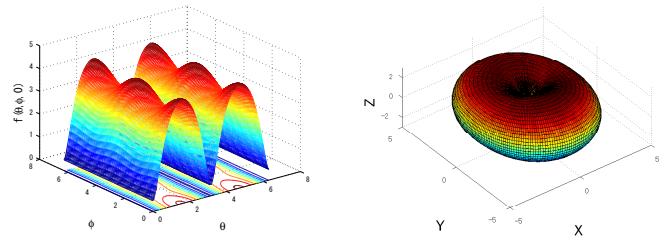

Fig. 1. True function $f(\theta, \phi, t)$ at time $t = 0$ (left) and the corresponding 3D shape of red blood cell (right).
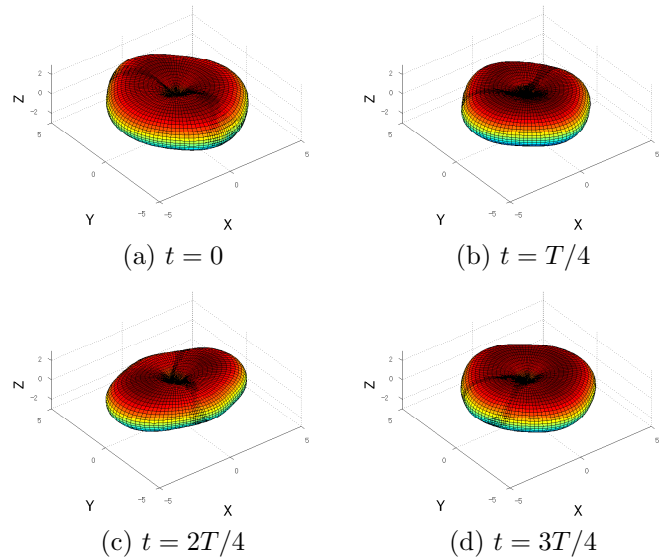

(a) $t = 0$

(b) $t = T/4$

(c) $t = 2T/4$

(d) $t = 3T/4$

Fig. 2. Sample plots of 3D shapes of deforming red blood cell reconstructed by optimal periodic smoothing spline $x(\theta, \phi, t)$.
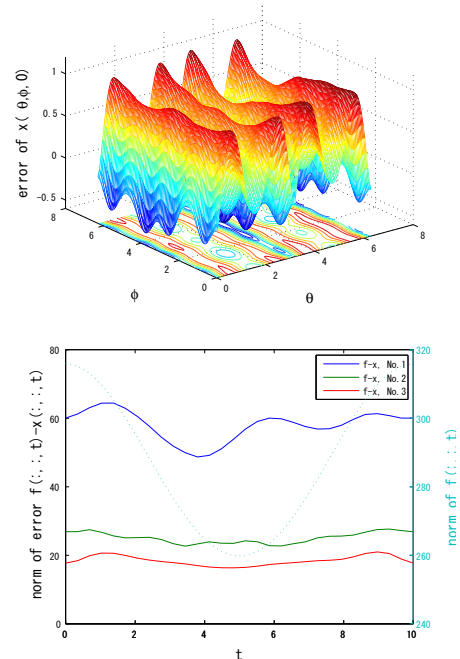

Fig. 3. Approximation error $f(\theta, \phi, t) - x(\theta, \phi, t)$ at $t = 0$ (top) and the error norms evaluated for each t (blue, green and red lines) (bottom).
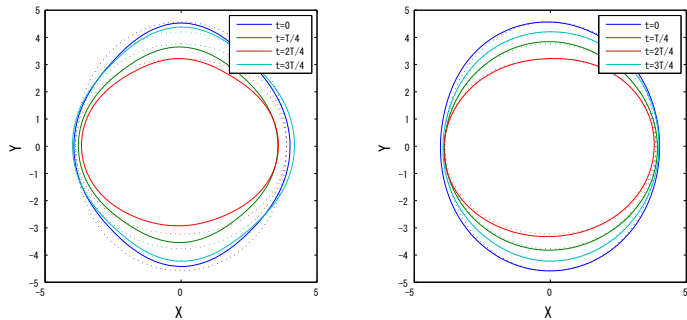
Fig. 4. XY-plane profile of constructed 3D shape of the red blood cell plotted at time $t = 0, T/4, 2T/4, 3T/4$: The case of $N_1 = N_2 = 5, N_3 = 10$ (left) and $N_1 = N_2 = 20, N_3 = 40$ (right).

the basis functions. Such splines are useful particularly for modeling dynamic shape of deformable objects by using two variables for 3D shape and one for time evolution. The trivariate splines are constructed as a tensor product of three B-splines, and an optimal smoothing spline problem is solved together with typical examples of constraints as periodicity.

Note that the splines are optimized for fixed knot points but the smoothing parameter will be adjusted by employing the generalized cross validation method. The problem is formulated as convex QP problem in such a way that a MATLAB QP solver is applicable for numerical solutions by converting 3D control point array to a vector.

The overall process of QP problem formulation is derived so that the general n-variate case,

$$x(t) = \sum_{i_1=-k}^{m_1-1} \cdots \sum_{i_n=-k}^{m_n-1} \tau_{i_1,i_2,\cdots,i_n} \prod_{j=1}^{n} B_{k,i_j}^{[j]}(t_j)$$

is easily deduced. We demonstrated the usefulness of the method by dynamic shape modeling of red blood cell, where we see that relatively small number of observation data yield satisfactory results. Further studies are needed to derive algorithms for shape preserving splines and splines incorporating various types of other constraints.

REFERENCES

E. B. Ameur, D. Sbibih and C. Leger, New Spline Quasi-Interpolant for Fitting 3-D Data on the Sphere: Applications to Medical Imaging, *IEEE Signal Processing Letters*, Vol. 14, No.5, pp.333-336, 2007.

A. A. Amini, Y. Chen, M. Elayyadi and P. Radeva, Tag surface Reconstruction and Tracking of Myocardial Beads from SPAMM-MRI with Parametric B-Spline Surfaces, *IEEE Trans. Medical Imaging*, vol. 20, no.2, 2001.

I. J. Anderson, M. G. Cox and J. C. Mason, Tensor-product spline interpolation to data on or near a family of lines, *Numerical Algorithms*, Vol. 5, pp.193-204, 1993.

A. Blake and M. Isard, *Active Contours*, Springer, 2000.

C. de Boor, *A practical guide to splines*, Revised Edition, Springer-Verlag, New York, 2001.

P. Brigger, J. Hoeg and M. Unser, B-Spline Snakes: A Flexible Tool for Parametric Contour Detection, *IEEE Trans. Image Processing*, Vol.9, No.9, pp.1484–1496, 2000.

M. Egerstedt and C. Martin, *Control theoretic splines: Optimal control, Statistics and Path Planning*, Princeton University Press, Princeton, NJ, 2010.

H. Fujioka, H. Kano, M. Egerstedt and C. Martin, Smoothing Spline Curves and Surfaces for Sampled Data, *Int. J. of Innovative Computing, Information and Control*, Vol.1, No.3, pp.429-449, 2005.

H. Fujioka and H. Kano, Periodic Smoothing Spline Surface and Its Application to Dynamic Contour Modeling of Wet Material Objects, *IEEE Transactions on Systems, Man, and Cybernetics- part A*, Vol.39, No.1, pp.251-261, 2009.

H. Fujioka and H. Kano, Recursive Construction of Optimal Smoothing Spline Surfaces with Constraints, *Preprints of The 18th IFAC World Congress*, pp.2278-2283, Milan, Italy, Aug. 28 - Sept. 2, 2011.

C. Habermann and F. Kindermann, Multidimensional Spline Interpolation: Theory and Applications, *Computational Economics*, Vol.30, Issue 2, pp.153-169, 2007.

F. Jaillet, B. Shariat, D. Vandorpe, Periodic B-Spline Surface Skinning of Anatomic Shapes, *Proc. of the 9th Canadian Conf. on Computational Geometry*, pp. 199-210, Kingston, Ontario, Canada, Aug.11-14, 1997.

H. Kano, H. Nakata and C. Martin, Optimal curve fitting and smoothing using normalized uniform B-splines: A tool for studying complex systems, *Applied Mathematics and Computation*, 169, issue 1, pp.96-128, 2005.

H. Kano, H. Fujioka, M. Egerstedt and C.F. Martin, Optimal Smoothing Spline Curves and Contour Synthesis, *Proc. of the 16th IFAC World Congress*, Prague, Czech Republic, July 4-8, 2005.

H. Kano, M. Egerstedt, H. Fujioka, S. Takahashi and C.F. Martin, Periodic Smoothing Spline, *Automatica*, Vol.44, No.1, pp.185-192, 2008.

H. Kano, H. Fujioka and C. F. Martin, Optimal smoothing and interpolating splines with constraints, *Applied Mathematics and Computation*, Vol.218, Issue 5, pp.1831-1844, 2011.

A. Karlsson, J. He, J. Swartling and S. Anderson, Numerical Simulations of Light Scattering by Red Blood Cells, *IEEE Trans. Biomedical Engineering*, Vol.52, No.1, pp.13-18, 2005.

M. J. Lai and L. L. Schumaker, *Spline Functions on Triangulations*, Cambridge University Press, 2007.

P. Lancaster and M. Tismenetsky, *The Theory of Matrices*, Second Edition, Academic Press, 1985.

J. R. Magnus and H. Neudecker, *Matrix Differential Calculus with Applications in Statistics and Econometrics*, Revised Edition, John Wiley and Sons, 1999.

T. Martin, E. Cohen, R.M. Kirby, Volumetric parametrization and trivariate B-spline fitting using harmonic functions, *Computer Aided Geometric Design*, Vol.26, pp.648-664, 2009.

T. Peng and R. F. Murphy, Image-Derived, Three-dimensional Generative Models of Cellular Organization, *Cytometry Part-A*, Vol.79, No.5, pp.383–391, 2011.

C. Pozrikidis, Numerical Simulation of the Flow-Induced Deformation of Red Blood Cells, *Annals of Biomedical Engineering*, Vol.31, pp.1194-1205, 2003.

G. Wahba, *Spline models for observational data*, CBMS-NSF Regional Conference Series in Applied Mathematics, 59, Society for Industrial and Applied Mathematics (SIAM), Philadelphia, PA, 1990.